

# A Smart Measurement and Stimulation System to Analyze and Promote Non-Nutritive Sucking of Premature Babies

Miguel Dias Pereira<sup>1,2</sup>, Octavian Postolache<sup>1,2</sup>, Pedro Silva Girão<sup>1</sup>

<sup>1</sup>Telecommunications Institute, Technical Institute of Lisbon, Lisbon, Portugal, joseper@est.ips.pt

<sup>2</sup>Polytechnic Institute of Setúbal, ESTS, LabIM, Setúbal, Portugal

**This paper presents a complete system that can be used to measure and to stimulate sucking abilities of premature babies. The system integrates measurement and stimulation capabilities that can be used separately or together. The sensing unit includes mainly a pressure sensor, a conditioning circuit and a microcontroller device. The stimulation unit includes a miniature and low-cost pneumatic pump, an electro-valve, and a conditioning circuit. The microcontroller is shared by both units. The system's software includes a routine that is used to define the waveform parameters of the synthesized pressure signals, a wavelet based routine that is used to process measurement data and a software component to perform fault detection and diagnosis. The system capabilities include self-calibration and self-testing. Throughout the paper several implementation details and experimental results will be presented and discussed.**

**Keywords:** Sucking pressure measurement, sucking stimulation, premature babies

## 1. INTRODUCTION

**T**HERE ARE several studies that justify a careful attention to the sucking activities in premature babies [1]-[4]. The detection of readiness conditions to a successful oral feeding of premature babies (PB) is relevant information for their autonomous survival capabilities [5]-[7]. Moreover, an abnormal sucking pattern may be an indication that the infant's neurological development is not progressing normally and may be the first symptom of disability [8]. In neonatology health care units, the intensive clinical support that is required by a PB is a matter of concern that affects directly the birth survival rate. However, if the average period that each PB stays in the intensive care neonatology unit is excessive, the number of available incubators reduces and the life support required by other PB is compromised or at least negatively affected. Hence, minimizing the costs and reducing the intensive care period required by a PB is a fundamental issue to optimize human and equipment resources in a neonatology unit.

The neonatal oral-motor assessment scale (NOMAS [9]-[10]) is the traditional method used to assess non-nutritive sucking (NNS) and nutritive sucking (NS) activities. This method has an intrinsic non-invasive nature because it is based on visual observations of sucking activities. However, there is little information about the method's reliability and the accessible results are qualitative and very dependent on the observer's skill and experience. Moreover, NOMAS is not a reliable method to detect several sucking abnormalities such as variations in sucking burst duration, inter-burst periods and sucking amplitude and frequency [11].

In a previous paper [12], the authors have already proposed a non-invasive measurement system to measure the NNS of a PB. However, the proposed measurement system does not include any stimulation unit that can be very important for speeding-up the sucking capabilities [13]-[15], and its reliability is compromised since it does not include any self-calibration, self-testing or fault

detection mechanisms. Regarding software improvements, the proposed pressure measurement and stimulation system (PMSS) takes advantages of wavelet capabilities to analyze NNS activities and to evaluate their evolution over time. The PMSS also includes wireless communication capabilities that can be used to centralize the surveillance of multiple PB that are in the same neonatology unit.

In regard to the specifications of the PMSS, it must be referred that they must comply with the main characteristics of the PB sucking signal, namely, a typical pressure amplitude between 500 Pa and 5000 Pa, a typical frequency between 0.5 Hz and 2 Hz, and a typical number of suctions per burst between 8 and 12 [11].

It is important to remark that there exist commercial data acquisition [16]-[19] and telemetry [20] solutions that can be used to implement a measurement system with similar, but not identical, characteristics of the one that is proposed in this paper. Those solutions are proprietary, their cost is excessively high, in the order of some thousands of USA dollars, and, above all, they don't provide an integrated solution to measure and stimulate sucking activities with a user friendly interface. In addition, the proposed PMSS includes two interesting capabilities, to mimic pressure signal (PS) and to analyze data sucking evolution by using the wavelet signature of the sucking patterns.

The paper is organized as follows: section I contains the paper's introduction; section II includes PMSS description, namely its hardware and software parts, the description of PMSS self-calibration, self-testing and fault detection mechanisms; section III is devoted to experimental results and section IV includes the paper's conclusion.

## 2. SYSTEM DESCRIPTION

This section describes the main components of PMSS hardware and software. The PMSS hardware includes two main parts, the pneumatic part and the electrical part. The software part includes several routines that are used to

define the waveform parameters of the synthesized PS, and also to perform data processing, self-calibration, self-testing and fault diagnosis tasks.

### A. Hardware

The hardware involves pneumatic and electrical elements. The pneumatic elements include a pneumatic pump, an electro-valve, a pressure sensor, a silicone pacifier and the pneumatic connections between those elements, namely, tubes, bifurcations and connectors. The electrical elements implement signal conditioning, data processing and wireless data transmission tasks. Those elements are a microcontroller, a Bluetooth interface transceiver, some operational amplifiers and electrical components.

#### A.1. Pneumatic Part

Fig.1 represents the pneumatic diagram of the PMSS. The main characteristics of the pneumatic devices are as follows: the pneumatic pump (PP) requires a 3.3 V nominal power supply voltage and it delivers a maximum output pressure equal to 103.4 kPa; the electro-valve has similar power supply requirements (3.3 V) and it has a maximum flow amplitude equal to 1 l/s; the pressure transducer [21] is a temperature compensated device that has a relative pressure measuring range equal to  $\pm 6.665$  kPa, a typical sensitivity equal to 0.3 mV/Pa, and a linearity error lower than 0.8 % of the measuring range amplitude. An additional miniature pressure transducer (PTR) can be included in the PMSS for fault detection and diagnosis purposes. It is also important to refer that the pneumatic pump includes an electrical switch ( $S_{PP}$ ) that is closed if the pump is running properly.

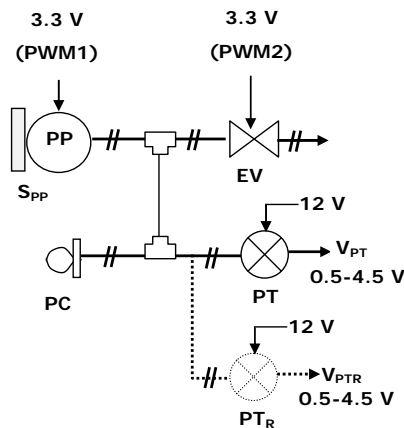


Fig.1. Pneumatic diagram of the pressure measurement and stimulation system (PP- pneumatic pump, EV- electro-valve, PT- pressure transducer,  $PT_R$ - redundant pressure transducer,  $S_{PP}$ - pneumatic pump switch, PC- pacifier).

The PP and the EV are controlled using a pulse width modulation (PWM) signal, which means that the signals that are represented in the pneumatic diagram are used to modulate the pressure variations generated by the pneumatic pump (PP) and by the electro-valve [22] that are used to increase or decrease the pressure amplitude values, respectively.

Fig.2 depicts the main components of the pneumatic part of the PMSS.

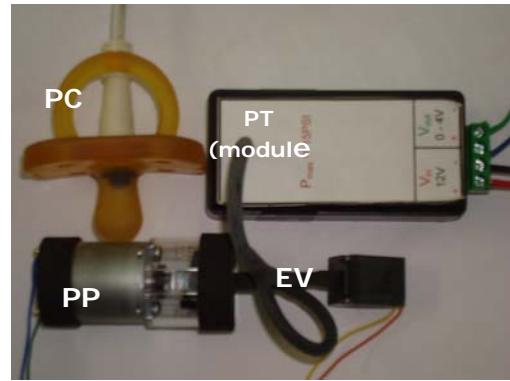


Fig.2. Main pneumatic elements of the pressure measurement and stimulation system.

#### A.2. Electrical Part

The main components of the electrical part of the PMSS include a microcontroller (PIC16F876), a RS-232 USART [23], and a Bluetooth-TTL protocol converter (MDFLY) [24] that assures the wireless communication capabilities of the PMSS. The microcontroller includes a 10-bit resolution A/D converter with 8 multiplexed input channels, 2 analog comparators and a programmable on-chip voltage reference generator. According to the PS characteristics, namely its output voltage range between 0.5 V and 4.5 V, the pressure measuring resolution that is given by the quotient between the ADC resolution and the PT sensitivity, is lower than 15 Pa. The microcontroller also includes 2 capture/compare PWM inputs with 16 bit resolution and three 16 bit timers.

The pulse width modulation signals, PWM1 and PWM2, are used to adjust the amplitude and the frequency of the pneumatic signal. Under normal working conditions, the pneumatic signal pressure can be adjusted between 0 Pa and 2000 Pa and its frequency can be adjusted between 0 Hz (constant amplitude) and a maximum frequency of 10 Hz. The RS-232 interface transceiver, which requires a voltage power supply amplitude between +3.0V and +5.5V, includes a dual charge pump and assures a transmission data rate up to 250 kbps using the standardized voltage levels of the RS-232 protocol. The Bluetooth-TTL transceiver module is entirely designed for RS-232 communication and its main characteristics include a nominal power supply voltage of 3 V, maximum power consumption lower than 210 mW, a typical RF transmitter power of +2 dBm and a typical receiver sensitivity of -80 dBm for a 0.1 % bit error rate (BER). This transceiver module allows a Bluetooth based wireless communication between the PMSS unit and a nursery vigilance center.

It is important to note that the signal conditioning (SC) circuit of the measurement system includes signal filtering and programmable gain amplification (PGA) capabilities. The gain of the PGA is controlled by the microcontroller using a digital potentiometer. Using this feature, it is possible to improve the measurements' resolution. Regarding the power consumption of the PP and the EV, these devices had a maximum current peak equal to 100 mA and 20 mA when powered with a 3.3 V supply voltage that corresponds to peak power consumption equal to 330 mW and 66 mW, respectively.

Fig.3 and Fig.4 show, respectively, the electrical schematic of the PMSS and the printed circuit board (PCB) that was implemented.

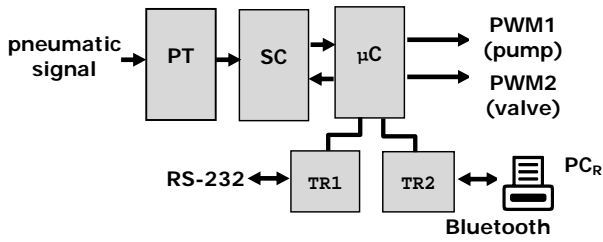


Fig.3. Electrical block diagram of the pressure measurement and stimulation system (PT- pressure transducer; SC- signal conditioning;  $\mu$ C- microcontroller; TR1- RS-232 transceiver; TR2- Bluetooth transceiver; PC<sub>R</sub>- remote personal computer).

The remote PC performs all software tasks that require higher processing capabilities than the ones provided by the microcontroller.

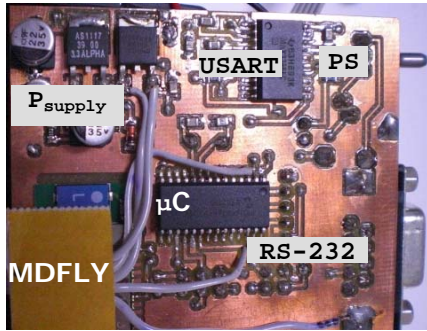


Fig.4. Pressure measurement and stimulation system PCB.

### B. Software

The software of the PMSS is organized in three modules: one is related to the synthesis of the pressure signals, according to the user requirements, namely, pressure amplitude, frequency, inter-burst period and other parameters that define the waveform characteristics of the sucking stimulus signal; another is a wavelet based data processing routine developed to identify sucking patterns and to analyze their evolution over time; and a third is related to PMSS calibration, self-testing and fault detection tasks.

Additional software routines were also developed for peak detection of the pressure signals and for configuration purposes. Configuration tasks include the definition of the following parameters: the threshold amplitude of the pressure signals to start data acquisition; the number of pressure peaks and sucking bursts that are used for data processing; the data sampling rate; the number of samples collected before and after each sucking burst and the statistical parameters that are used for data processing of measurement data. The PMSS software also implements a database that stores, on a weekly basis, the quadratic average of the wavelet coefficients that are obtained for each PB under observation. The analysis of the database contents

is essential to analyze the evolution of NNS sucking parameters and to detect abnormal sucking patterns.

#### B.1. Pressure Signal Synthesis

Basically, there are two methods to synthesize the pressure signals that are used for sucking stimulation purposes: they can be generated according to pre-defined patterns or they can be defined according the waveforms of the sucking pressure signals generated during NNS activities. In the first case, the pressure signal ( $s(t)$ ) is basically a trapezoidal amplitude modulated signal that is defined according to the following relations,

$$s(t) = s(t + k \cdot T_{IB})$$

$$s(t) = m(t) \cdot \sin\left(\frac{2 \cdot \pi \cdot t}{T_0}\right)$$

$$m(t) = \begin{cases} \frac{S_{amp}}{T_R} \cdot t & \text{if } 0 \leq t < T_R \\ S_{amp} & \text{if } T_R \leq t < T_R + T_D \\ S_{amp} \cdot \left[1 - \frac{1}{T_F} \cdot (t - (T_R + T_D))\right] \frac{S_{amp}}{T_R} \cdot t & \text{if } T_R + T_D \leq t < T_R + T_D + T_F \end{cases} \quad (1)$$

where  $S_{amp}$  represents the amplitude of sucking signal between rising and falling phases,  $T_0$  represents the sucking period,  $f_0 = 1/T_0$  is the sucking frequency,  $T_R$  and  $T_F$  are the rise and fall time of the sucking signal,  $T_D + T_R + T_F$  represents the period of the sucking signal,  $T_{IB}$  represents the inter-burst period and  $K$  is an integer number.

All the coefficients that define the sucking stimulation signal, including the inter-burst period, can be adjusted during program execution.

Fig.5 represents an example of a synthesized sucking pattern signal.

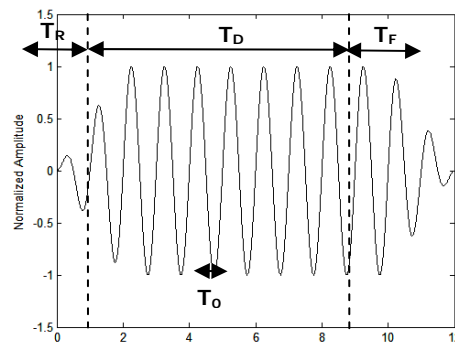


Fig.5. Sucking pattern signal that is synthesized with the following set of coefficients:  $T_0=1$  s ( $f_0=1$  Hz);  $T_R=2$  s;  $T_F=2$  s and  $T_D=8$  s.

The second method to synthesize pressure signals is based on the NNS signals that are captured during sucking activities. In this case the synthesized pressure signal mimics the NNS signal generated by the PB. It is possible, without modifying the NNS signal profile, to modify its amplitude, frequency and inter-burst period.

According to data processing requirements, namely the accuracy that is required to detect the amplitude and timing parameters of the suction peaks, the number of suction per burst (suction frequency) and eventual suction anomalies

that are contained in the NNS signal, it is possible to select one out of two sampling modes. The sampling frequencies that are used for each sampling rate, are defined by,

$$\begin{aligned} f_{OS} &= 10 \cdot f_N \quad (\text{oversampling mode}) \\ f_{NS} &= 2 \cdot f_N \quad (\text{Nyquist ampling mode}) \end{aligned} \quad (2)$$

where  $f_N$  represents the Nyquist frequency whose value, according to the characteristics of the suction signal, is considered to be equal to 5 Hz.

By default, the oversampling mode uses an oversampling coefficient equal to 10, which means that the sampling rate is equal to ten times the Nyquist rate.

### B.2 Sucking Pattern Recognition Using Wavelets

There are several characteristics of the wavelet transforms [25] that are particularly interesting to perform the characterization of sucking signals. These characteristics include the non-existence of a compromise between time and frequency resolutions, and the inherent capability to detect the signal trends, breakdowns and sharp peak variations. Moreover, wavelets have the capability to perform the signal compressing and de-noising with a minimal distortion. The wavelet signal compression capability is particularly important in data storage and transmission.

The wavelet coefficients obtained from the suction pattern signals can be used to detect abnormal conditions of the NNS signal, to identify the NNS source (sucking signature) and to trace the evolution of sucking signatures of each PB over time.

As an example, Fig.6 represents the scalogram for a simulated sucking signal that includes 4 burst sucking patterns with the following temporal sequence of frequencies and amplitudes: freq=2.5 Hz and amplitude=1; freq=5 Hz and amplitude=1; freq=12.5 Hz and amplitude=10; freq=2.5 Hz and amplitude=1 and freq=2.5 Hz and amplitude=1.

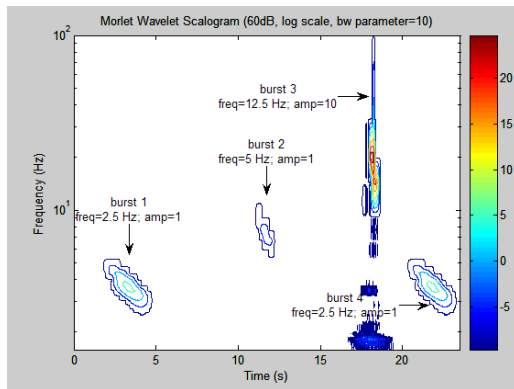


Fig.6. Scalogram for a simulated sucking signal that includes 4 burst sucking patterns.

As expected, the graph confirms a clear correlation between the simulated sucking signal and the correspondent scalogram, which confirms that the wavelet transforms are an efficient data processing tool to characterize NNS

patterns. It is important to note that this data processing tool does not require the use of peak detection algorithms that exhibit a higher processing load, a lower accuracy and a higher risk of false detections caused by low values of the signal to noise ratio (SNR).

### C. Self-Calibration, Self-Testing and Fault Detection

Pneumatic systems are inherently non-linear. In this case, the non-linearity is due to the pneumatic pump characteristic that can be higher than 20 % of its full scale range. Hence, a progressive polynomial calibration technique [26]-[29], using three calibration points, was used to perform the linearization of the relationship between the output pressure of the pneumatic pump ( $p$ ) and the voltage that is applied to its input ( $V_m$ ). So, using the function,  $p(V_m)$  according to the following set of conditions,

$$\begin{cases} p = 0 & \text{if } V_m = 0 \\ p = p_M/2 & \text{if } V_m = V_M/2 \\ p = p_M & \text{if } V_m = V_M \end{cases} \quad (3)$$

where  $V_M$  and  $p_M$  represent the maximum input voltage and output pressure of the pneumatic pump, respectively, and  $V_M/2$  and  $p_M/2$  represent their midrange values, respectively.

This set of conditions assures a linearization of the pneumatic pump characteristic canceling its offset, gain and the second order linearity error of its midrange pressure. The recursive calibration functions that cancel each one of the previous errors are given by [26]-[27],

$$\begin{cases} p_{c3}(V_m) = p_{c2}(V_m) + \alpha_3 \cdot p_{c1}(V_m) \cdot [p_{c2}(V_m) - p_M] \\ p_{c2}(V_m) = p_{c1}(V_m) + (1 + \alpha_2) \\ p_{c1}(V_m) = p(V_m) + \alpha_1 \end{cases} \quad (4)$$

being the coefficients  $[\alpha_1, \alpha_2, \alpha_3]$ , defined by,

$$\begin{aligned} \alpha_1 &= -p(V_M = 0) \\ \alpha_2 &= \frac{p_M - p_{c1}(V_M)}{p_{c1}(V_M)} \\ \alpha_3 &= \frac{p_M/2 - p_{c2}(V_M/2)}{p_{c1}(V_M/2) \cdot [p_{c2}(V_M/2) - p_M]} \end{aligned} \quad (5)$$

where  $p(V_M=0)$  represents the output pressure offset of the pneumatic pump and the other parameters have the meaning previously defined.

In what concerns fault detection capabilities, the feedback nature of the PMSS can be easily used to detect and diagnose faults. Assuming that a fault detection routine is part of the microcontroller firmware and an additional (redundant) pneumatic transducer (PTR) is included in the PMSS, the application of specific voltage values ( $V_m$ ) to the PP and the measurement of the voltage values obtained from PT and  $PT_R$  can be used to diagnose fault conditions. For example, for  $V_m=V_M$  and  $S_{PP}$  detected closed, which means that PP is working properly, if the voltage values that are obtained from the pressure transducers are  $V_{PT}=0.5$  V (null

relative pressure) and  $V_{PTR} > 0.5$  V (positive relative pressure) when a close command is applied to the electro-valve, the conclusion is that PT is not working properly. In this case, the PMSS can continue to work properly if the redundant pressure transducer (PTR) becomes the working pressure transducer, removing the anomalous functioning transducer PT from the pneumatic circuit by using a cut-off electro-valve. Thus, the use of this kind of test procedures grants the system auto-test and fault diagnosis capabilities and can even improve its reliability.

### 3. RESULTS

This section includes some calibration and testing results of the PMSS. In what concerns on-line testing, two types of tests were performed, one related to NNS pressure measurement and another related to NNS pressure stimulation. As previously referred, the PMSS integrates measurement and stimulation capabilities that can be used separately or jointly; however, measurement and stimulation tests were considered separately to facilitate data analysis.

Fig.7 depicts the experiment set up that was used to perform on-line tests of the PMSS.



Fig.7. Experiment set up that was used to perform on-line tests of the PMSS.

#### A. Calibration results

After previous calibration of the pneumatic pump characteristic performed according to the progressive polynomial calibration method previously described, the calibration of the pressure transducer was carried out. The calibration was performed using the following set of instruments: a portable pneumatic tester [30]; an inclined U-tube manometer [31] and a digital multimeter [32]. The pressure measuring range used for calibration purposes varies between 0 Pa (no relative pressure) and 5000 Pa, and a constant pressure increment step of 50 Pa was used between adjacent calibration points. For each calibration point, a set of 1024 measurements was taken and the average value of the measurements was calculated in order to minimize random errors with null average values. The maximum voltage confidence interval, associated with each calibration point, is about 3.36 mV for a confidence level equal to 99.5 %.

Fig.8 represents the calibration results that were obtained.

The graph clearly shows a linear relation between the output voltage of the pressure transducer and its input pressure, the correlation coefficient between those variables

being almost equal to one ( $cc=0.999$ ). From the calibration results it is also possible to obtain a sensitivity value equal to 0.2953 mV/Pa and an offset error equal to 0.4601 mV for the characteristic of the transducer.

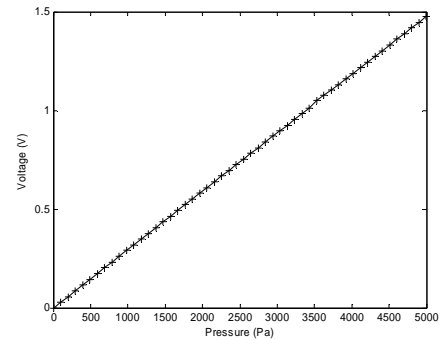


Fig.8. Pressure transducer calibration results.

#### B. On-line testing results

This section presents some experimental results of the PMSS using each one of its operating modes, namely, NNS measurement and NNS stimulation.

##### B1. NNS Measurement

Data acquisition was carried out using a pre-defined trigger threshold equal to 100 mV, that corresponds to a pressure threshold level almost equal to 30 Pa for the default PGA gain coefficient ( $gain=10$ ), and a middle-trigger [33] mode. A set of samples taken before and after each trigger are stored for data processing purposes. It is important to refer that the number of samples collected before and after the trigger event can be different if different risk levels are required to validate the start or the end of each sucking burst. For example, if a lower fault probability is required to detect the start of a sucking burst than the one to detect its end, the number of samples stored before the trigger event must be higher than the number of samples collected after the trigger event. The time period that was used to analyze the evolution of NNS capabilities was equal to three weeks. During this period several sucking bursts were stored on a weekly basis. Fig.9 represents the NNS pattern evolution throughout a period of three weeks. The weeks are numbered according to the PB gestational age.

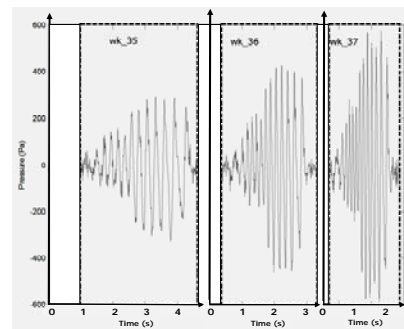


Fig.9. Typical NNS pattern evolution throughout a time period of three weeks.

From the graph, it is evident that the NNS amplitude and frequency increase over time, starting in the first week (wk\_35) from an amplitude and frequency values approximately equal to 300 Pa and 0.4 Hz, respectively, up to an amplitude and frequency approximately equal to 380 Pa and 0.8 Hz, respectively, in the third week (wk\_37). These results agree with the typical evolution of NNS activities that were obtained by other authors [34]-[35] using different measuring techniques, namely, using NOMAS video recording methods.

An easier interpretation of the evolution over time of the pressure sucking signals, in terms of amplitude and frequency, can be obtained using the scalogram of the pressure signal. Fig.10 represents the scalogram that was obtained using a quadratic average of the wavelet coefficients of multiple NNS sucking patterns collected during the period under analysis. During each week, a set of 512 sucking patterns were used to evaluate the averaged quadratic composition of the scalogram coefficients.

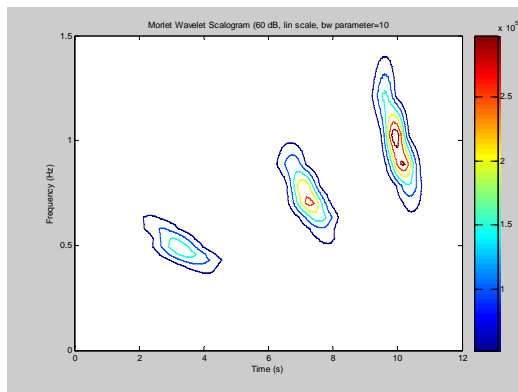


Fig.10. Scalogram of NNS sucking patterns collected during a time period of three consecutive weeks.

The scalogram clearly shows an increase over time of the amplitude and frequency of the NNS pattern. It is also important to underline that the time indexes associated with each trigger event were stored and can be used to evaluate other important parameters of the NNS patterns, namely, the number of suction per minute, the sucking burst rate, and the inter-burst sucking period.

## B2. NNS Stimulation

To obtain the main dynamic characteristics of the stimulation part of the PMSS a set of square wave electrical signals were used to actuate the pneumatic pump. During the higher amplitude period of the square wave signal ( $\text{amp}_H=4\text{ V}$ ) the pump is actuated and the pressure increases; conversely, during the lower amplitude period ( $\text{amp}_L=0\text{ V}$ ) the electro-valve is actuated and the pressure decreases. The output voltage that was obtained from the PT was digitized with a sampling rate of 5000 S/s. Fig.11 represents the normalized output pressure generated by the PP for a square wave input voltage ( $V_m$ ) with frequencies equal to 1 Hz (continuous line) and 10 Hz (dotted line). The normalization was performed relatively to the maximum output pressure generated by the PP.

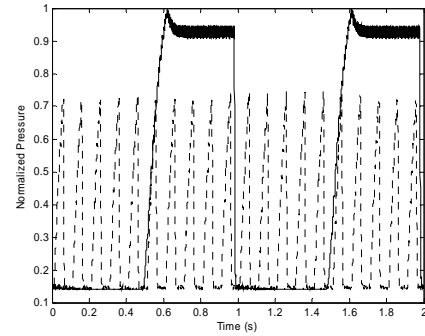


Fig.11. Normalized output pressure generated by the PP for a square wave PP input voltage (continuous line- 1Hz, dotted line- 10 Hz).

In order to obtain the low-pass characteristic of the stimulation part of the PMSS, a set of sinusoidal signals with offset and amplitude values equal to 2 V and frequencies equal to 0.1 Hz, 0.2 Hz, 0.5 Hz, 1 Hz, 2 Hz, 5 Hz, 10 Hz, 20 Hz and 50 Hz, were used. Fig.12 represents the Bode diagram that was obtained using a least mean square (LMS) curve fitting of the experimental data.

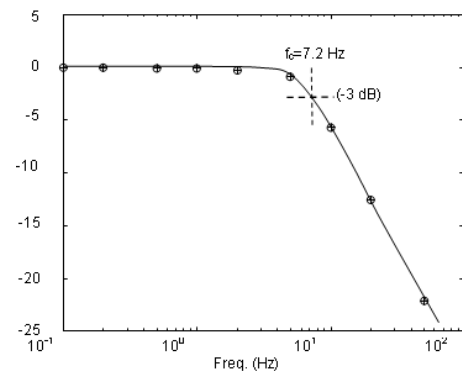


Fig.12. Bode diagram of the pressure measurement and stimulation system (circle symbol- experimental data, continuous line- LMS curve fitting of the experimental data).

The Bode diagram shows that the stimulation part of the PMSS exhibits a first order low-pass filter characteristic with a cutoff frequency ( $f_c$ ) approximately equal to 7.2 Hz. The low-pass frequency characteristic that was obtained confirms the exponential step response of a first order system. The time constant ( $\tau \approx 24,8\text{ ms}$ ) of the step response of the PMSS, which can be obtained from the results represented in Fig.11, is almost equal to the reciprocal of the cutoff frequency of the low-pass filter ( $f_c=1/2.\pi.\tau$ ). It is important to emphasize the fact that the value of the obtained cutoff frequency depends mainly on the characteristics of the pneumatic system, namely, on the values of air compressibility, and pneumatic tubes' lengths and sections.

## 4. CONCLUSION

This paper presented a smart measurement and stimulation system to analyze and promote NNS activities of PB. A low-cost and flexible solution based on commercial off-the-shelf (COTS) components and on a microcontroller was

implemented and several software programs were developed. A methodological approach based on wavelets is proposed to analyze NNS data, namely to evaluate the evolution over time of the amplitude and frequency of sucking patterns. The PMSS also possesses two additional smart sensing capabilities, self-calibration and self-testing, that improve its accuracy and reliability. The proposed system represents a feasible, reliable and low cost solution that can be used with an acceptable accuracy level in every neonatology health care unit.

## REFERENCES

- [1] Lau, C., Alagugurusamy, C., Schanler, R., Smith, E.O., Shulman, R.J. (2000). Characterization of the development stages of sucking in preterm infants during bottle feeding. *Acta Paediatrica*, 89, 846-852.
- [2] Lau, C., Schanler, R. (2000). Oral feeding in premature infants: Advantage of a self-paced milk flow. *Acta Paediatrica*, 89, 453-459.
- [3] Lau, C., Sheena, H., Shulman, T., et al. (1997). Oral feeding in low birthweight infants. *Journal of Pediatrics*, 130, 561-569.
- [4] Lundqvist, C., Hafström, M. (1999). Non-nutritive sucking in full-term and preterm infants studied at term conceptional age. *Acta Paediatrica*, 88, 1287-1289.
- [5] Thoyre, S., Shaker, C., Pridham, K. (2005). The early feeding skills assessment for preterm infants. *Neonatal Networks*, 24 (3), 7-16.
- [6] Pridham, K., Steward, D., Thoyre, S., Brown, R. (2007). Feeding skill performance in premature infants during the first year. *Early Human Development*, 83 (5), 293-305.
- [7] Gewolb, I., Bosma, J., Taciak, V., Vice, F. (2001). Abnormal developmental patterns of suck and swallow rhythms during feeding in preterm infants with bronchopulmonary dysplasia. *Development Medicine & Child Neurology*, 43 (7), 454-9.
- [8] Medoff-Cooper, B., Mcgrath, J., Bilker, W. (2000). Nutritive sucking and neurobehavioral development. *The American Journal of Maternal/Child Nursing*, 25 (2), 64-70.
- [9] Palmer, M., Crawley, K., Blanco, I. (1993). Neonatal oral-motor assessment scale: A reliability study. *Journal of Perinatology*, 13 (1), 28-34.
- [10] Palmer, M. (1993). Identification and management of the transitional suck pattern in premature infants. *Journal of Perinatal & Neonatal Nursing*, 7, 66-75.
- [11] Palmer, M. (1999). Developmental outcome for neonates with dysfunctional and disorganized sucking patterns: Preliminary findings. *Infant-Toddler Intervention: The Transdisciplinary Journal*, 3, 299-308.
- [12] Pereira, M.D., Viegas, V., Banha, C., Postolache, O., Girao, P.S. (2009). Advanced signal processing techniques to measure and classify non-nutritive suction of premature and newly born babies. In *Intelligent Data Acquisition and Advanced Computing Systems - IDAACS 2009*, 21-23 September 2009. IEEE, 63-66.
- [13] Fucile, S., Gisel, E., Lau, C. (2002). Oral stimulation accelerates the transition from tube to oral feeding in preterm infants. *Jornal de Pediatria*, 141 (2), 230-236.
- [14] Fucile, S., Gisel, E., Lau, C. (2005). Effect of an oral stimulation program on sucking skill maturation of preterm infants. *Developmental Medicine & Child Neurology*, 47 (3), 158-62.
- [15] Rocha, A., Moreira, M., Pimenta, H., et al. (2007). A randomized study of the efficacy of sensory-motor oral stimulation and non-nutritive sucking in very low birthweight infant. *Early Human Development*, 83 (6), 385-8.
- [16] ION Publications LLC (2008). NTrainer - new device helps premature babies get off feeding tubes better. <http://www.science20.com>.
- [17] Site of Care Systems (2011). Neonatal healthcare software. <http://www.siteofcare.com/products/nursery>.
- [18] ADInstruments (2010). Data acquisition systems. <http://www.adinstruments.com/products>.
- [19] BIOPAC Systems Inc. (2011). MP 150 system. <http://www.biopac.com/Research.asp?Pid=3641&Main=Systems>.
- [20] Millar Instruments, Inc. (2011). TRM telemetry systems. <http://millar.com/products/telemetry>.
- [21] Sensortechncs (2011). Honeywell. Temperature compensated pressure sensor, 40PC001B. <http://www.sensortechncs.com>.
- [22] HARTMANN. (2011). Tensoval - Blood pressure monitor for reliable upper arm measurement. <http://productcatalogue.hartmann.info>.
- [23] Maxim Integrated Products (2001). Transceiver for PDAs and cell phones. <http://datasheets.maxim-ic.com/en/ds/MAX3386E.pdf>.
- [24] MDFLY Electronics. (2011). Wireless bluetooth TTL transceiver module. [http://www.mdfly.com/index.php?main\\_page=product\\_info&products\\_id=63](http://www.mdfly.com/index.php?main_page=product_info&products_id=63).
- [25] Cristi, R. (2004). *Modern Digital Signal Processing*. Thompson Brooks/Cole.
- [26] Horn, G., Huijsing, J. (1998). *Integrated Smart Sensors, Design and Calibration*. Kluwer Academic Publishers.
- [27] Dias Pereira, J., Postolache, O., Girão, P. (2009). PDF-based progressive polynomial calibration method for smart sensors linearization. *IEEE Transactions on Instrumentation and Measurement*, 58 (9), 3245-3252.
- [28] Goes, F., Meijer, G. (1997). A simple accurate bridge-transducer interface with continuous autocalibration. *IEEE Transactions on Instrumentation and Measurement*, 46 (3), 704-710.
- [29] Simon, P., Vries, P., Middelhoek, S. (1996). Autocalibration of silicon Hall devices. *Sensors and Actuators A: Physical*, 52, 203-207.
- [30] AMETEK (2011). Portable pneumatic tester – model T730. [http://www.jofra.com/UK/Products/Pressure\\_calibrators.aspx?ProductID=PROD31&m=ecom\\_catalog](http://www.jofra.com/UK/Products/Pressure_calibrators.aspx?ProductID=PROD31&m=ecom_catalog).
- [31] JAZD Markets, Inc. (2011). Inclined U-tube mano - meter - model FL1.5. <http://www.jazdlifesciences.com>.

- [32] Keithley Instruments Inc. (2011). Digital Multimeter – model 2000. <http://www.keithley.com>.
- [33] Agilent Technologies (2011). Evaluating oscilloscope fundamental: Application note. <http://cp.literature.agilent.com/litweb/pdf/5989-8064EN.pdf>.
- [34] Mizuno, K., Ueda, A. (2003). The maturation and coordination of sucking, swallowing, and respiration in preterm infants. *The Journal of Pediatrics*, 142 (1), 36-40.
- [35] Medoff-Cooper, B., Bilker, W., Kaplan, J. (2001). Suckling behaviour as a function of gestacional age: A cross-sectional study. *Infant Behavior and Development*, 24, 83-94.

Received October 15, 2011.  
Accepted December 5, 2011.